



## RESEARCH ARTICLE

# Cytoprotective autophagy induction by withaferin A in prostate cancer cells involves GABARAPL1

Eun-Ryeong Hahm<sup>1</sup> | Shivendra V. Singh<sup>1,2</sup>

<sup>1</sup>Department of Pharmacology and Chemical Biology, University of Pittsburgh School of Medicine, Pittsburgh, Pennsylvania

<sup>2</sup>UPMC Hillman Cancer Center, University of Pittsburgh School of Medicine, Pittsburgh, Pennsylvania

**Correspondence**

Shivendra V. Singh, 2.32A UPMC Hillman Cancer Center Research Pavilion, 5117 Centre Avenue, Pittsburgh, PA 15213.  
Email: singhs@upmc.edu

**Funding information**

National Cancer Institute,  
Grant/Award Numbers: P30 CA047904, RO1 CA142604-10, RO1 CA225716-1A1

**Abstract**

Withaferin A (WA) is a naturally occurring steroidal lactone with proven cancer chemopreventive activity in preclinical models of different cancers including prostate adenocarcinoma. Previously we compared the RNA-seq data from control and WA-treated 22Rv1 human prostate cancer cells to identify mechanistic targets of this phytochemical. The Gene Ontology pathway analysis of the RNA-seq data revealed significant upregulation of genes associated with autophagy upon WA treatment in 22Rv1 cells. In this study, we extended these findings to investigate the mechanism underlying WA-induced autophagy. Initially, we confirmed autophagy induction by WA treatment by transmission electron microscopy using three prostate cancer cell lines (LNCaP, 22Rv1, and PC-3). Fourteen common genes altered by 8- and 16-hour exposure to WA were identified from human autophagy PCR array and these results were consistent with the RNA-seq data. Two key autophagy markers (LC3BII and SQSTM1) were robustly increased in WA-exposed LNCaP, 22Rv1, and PC-3 cells as determined by immunoblotting, and this effect was elevated in the presence of autophagy inhibitor bafilomycin A1 (BafA1). BafA1 treatment augmented WA's cytotoxicity and subsequently its proapoptotic potential. WA treatment induced GABARAPL1 (ATG8L) protein expression in all three cell lines and its knockdown by RNA interference attenuated WA-mediated apoptosis. WA-induced autophagy was not affected in the presence of an antioxidant (EUK134). Taken together, the present study reveals that WA-mediated autophagy is cytoprotective and mediated by GABARAPL1.

**KEYWORDS**

autophagy, chemoprevention, prostate cancer, withaferin A

## 1 | INTRODUCTION

Prostate cancer remains a major health concern for American men.<sup>1</sup> One of the commonly used treatment options for this disease is androgen deprivation therapy (ADT).<sup>2</sup> However, patients on ADT ultimately experience development of castration-resistant prostate

cancer (CRPC) that has a very poor prognosis.<sup>2</sup> Nguyen et al<sup>3</sup> showed that autophagy is stimulated during ADT as a survival mechanism to escape hormone-deficient environment subsequently promoting CRPC development. Unlike other carcinomas, prostate cancer preferentially utilizes lipids for cell growth and survival.<sup>4</sup> Some studies showed the connection between autophagy and lipid metabolism in

**Abbreviations:** 3-MA, 3-methyl adenine; ADT, androgen deprivation therapy; ANOVA, analysis of variance; AR, androgen receptor; ARE, antioxidant responsive element; BafA1, bafilomycin A1; CRPC, castration-resistant prostate cancer; C<sub>t</sub>, threshold cycle; DMSO, dimethyl sulfoxide; EMT, epithelial-mesenchymal transition; GAPDH, glyceraldehyde 3-phosphate dehydrogenase; GO, Gene Ontology; NRF2, NF-E2-related factor 2; PARP, poly(ADP-ribose) polymerase; PBS, phosphate-buffered saline; PI, propidium iodide; PTEN, phosphatase and tensin homolog; ROS, reactive oxygen species; siRNA, small interfering RNA; TCGA, The Cancer Genome Atlas; TRAMP, TRansgenic Adenocarcinoma of Mouse Prostate; WA, withaferin A.

prostate cancer survival, explaining that during ADT, lipid droplets rich in prostate cancer cells are sequestered in autophagosome and ultimately utilized for energy production and cell survival.<sup>5,6</sup> Autophagy was shown to be required for phosphatase and tensin homolog (PTEN)-loss driven prostate cancer.<sup>7</sup> As dysregulation of autophagy is implicated in prostate cancer, the modulators of this process are currently being evaluated in clinical trials, but their lack of specificity and cytotoxicity to normal tissues are still major concerns for therapeutic purposes.<sup>8</sup> Because prostate cancer has a long latency and its risk factors are not easily modifiable, chemoprevention represents an attractive alternate for decreasing the mortality and morbidity from this disease. Several large prostate cancer chemoprevention trials, including PCPT, REDUCE, and SELECT have been conducted but their outcomes were not promising.<sup>9-11</sup> Therefore, a safe and efficacious intervention for prostate cancer chemoprevention is still a clinically unmet need.

Withaferin A (WA), which is a steroidal lactone derived from a medicinal plant (*Withania somnifera*) commonly known as Ashwagandha, appears encouraging for treatment and/or prevention of cancer.<sup>12</sup> Yang et al<sup>13</sup> were the first to demonstrate WA-mediated inhibition of PC-3 human prostate cancer xenograft growth in vivo. These investigators also reported that the tumor proteome was an important mechanistic target of WA.<sup>13</sup> In another study, WA was shown to induce Par-4-dependent apoptosis in androgen-refractory prostate cancer cells and these effects were abrogated by over-expression of androgen receptor (AR).<sup>14</sup> Inhibition of prostate cancer cell viability in the presence of WA is also associated with cell cycle arrest.<sup>15</sup> Two studies showed chemoprevention of prostate cancer development in TRansgenic Adenocarcinoma of Mouse Prostate (TRAMP) and PTEN-deleted transgenic mouse models.<sup>16,17</sup> One of the desired characteristics of potential chemopreventive interventions is cancer cell-selective mechanisms. WA was shown to selectively induce cell death in androgen-independent PC-3 and DU145 human prostate cancer cells but not in normal fibroblasts.<sup>18</sup> An azido derivative of WA (3-AWA) was shown to induce apoptosis and inhibit epithelial-mesenchymal transition (EMT) in prostate cancer cells.<sup>19</sup> We reported recently that WA treatment suppresses fatty acid metabolism in LNCaP and 22Rv1 cells in vitro and neoplastic cells of the prostate in vivo in Hi-Myc transgenic mice.<sup>20</sup> Collectively, these studies demonstrate therapeutic as well as chemopreventative potential of WA with no toxicity to normal cells in vitro or in vivo.<sup>16-18</sup> These studies suggest that it may be worthwhile to investigate the mechanisms underlying anticancer effect of WA.

In a prior publication from our laboratory, we compared RNA-seq data from control and WA-treated 22Rv1 cells to identify novel mechanistic targets of this phytochemical in prostate cancer.<sup>20</sup> The Gene Ontology (GO) pathway analysis of the RNA-seq data from WA-treated 22Rv1 cells revealed upregulation of genes associated with autophagy when compared to solvent-treated control cells.<sup>20</sup> The goal of the present study was to investigate the mechanism underlying WA-mediated autophagy in prostate cancer. The present study reveals that WA-induced autophagy is cytoprotective in prostate cancer cells and mediated, at least in part, by GABARAPL1.

## 2 | MATERIALS AND METHODS

### 2.1 | Reagents

WA (purity > 95%) was purchased from ChromaDex (Irvine, CA), dissolved in dimethyl sulfoxide (DMSO; 20 mM stock), and stored at  $-80^{\circ}\text{C}$ . The 3-methyl adenine (3-MA) was from Sigma-Aldrich (St Louis, MO). Bafilomycin A1 (BafA1) and EUK134 were from Selleckchem (Houston, TX). Anti-glyceraldehyde 3-phosphate dehydrogenase (GAPDH) antibody was from GeneTex (Irvine, CA). Antibodies against LC3B, SQSTM1, cleaved poly(ADP-ribose) polymerase (PARP), and cleaved caspase-3 were from Cell Signaling Technology (Danvers, MA). An antibody against GABARAPL1 was from Proteintech (Rosemont, IL). Nonspecific control small interfering RNA (siRNA) and GABARAPL1-targeted siRNA were purchased from Qiagen (Valencia, CA) and Santa Cruz Biotechnology (Dallas, TX), respectively.

### 2.2 | Cell culture

The PC-3, LNCaP, and 22Rv1 cells were obtained from the American Type Culture Collection (Manassas, VA) and cultured as instructed by the supplier. These cell lines were last authenticated by us in March of 2017.

### 2.3 | GO enrichment analysis

Our previous RNA-seq data (NCBI accession number GSE137519) was used for the GO enrichment analysis.<sup>20</sup>

### 2.4 | Transmission electron microscopy

LNCaP, 22Rv1, and PC-3 cells were treated with DMSO (control) or  $2\ \mu\text{M}$  WA for 16 hours and then the cells were washed with phosphate-buffered saline (PBS) and fixed in 2.5% glutaraldehyde solution. Sections were imaged with the use of JEOL 1011 transmission electron microscope at  $\times 25\ 000$  magnification and autophagic vacuoles were quantitated as previously described.<sup>21</sup>

### 2.5 | Human autophagy PCR array

The 22Rv1 human prostate cancer cells were seeded at a density of  $1.5 \times 10^6$  cells in 100-mm dish in triplicate, allowed to attach by overnight incubation, and then treated with DMSO (control) or  $2\ \mu\text{M}$  WA for 8 or 16 hours. The cells were harvested by trypsinization and total RNA was extracted using the RNeasy Mini Kit (Qiagen) following the instructions of the vendor. Reverse transcription was performed using  $1\ \mu\text{g}$  of total RNA and RT<sup>2</sup> First-Strand Kit (Qiagen) following the supplier's protocol. To evaluate the effect of WA treatment on the levels of genes involved in

autophagy, the Human Autophagy RT<sup>2</sup> Profiler PCR Array (Qiagen) was used. The mixtures of complementary DNA and RT<sup>2</sup> SYBR Green ROX qPCR Mastermix (Qiagen) were prepared immediately before the real-time polymerase chain reaction (PCR). After brief centrifugation, 25  $\mu$ L of the mixtures was loaded into each well of the PCR array plate (96-well format) provided by the manufacturer. Real-time PCR was performed in a two-step cycling program by the use of an ABI StepOnePlus; 10 minutes at 95°C followed by 40 cycles of 15 seconds at 95°C and 1 minute at 60°C. The data were analyzed using the web-based software provided by the manufacturer. The threshold cycle ( $C_t$ ) was calculated, and the genes with  $C_t$  values above 35 were considered undetected. Baseline and threshold values were set manually at the same level for all the samples to allow comparison of multiple plates. The  $C_t$  value of each gene was adjusted for the average  $C_t$  of the house-keeping genes to generate  $\Delta C_t$  values. The  $\Delta\Delta C_t$  values were calculated as the difference in  $\Delta C_t$  between control and treated samples for the basal gene expression levels.

## 2.6 | Western blot analysis

Cells ( $4 \times 10^5$  cells/6-cm dish for PC-3 and LNCaP and  $7.5 \times 10^5$  cells/6-cm dish for 22Rv1) were treated with DMSO (control) or reagents including 2  $\mu$ M WA or 3 nM BafA1 or 30  $\mu$ M EUK134 for specified time periods. In certain experiments, 22Rv1 cells were transiently transfected with 100 nM control siRNA or 100 nM GABARAPL1-targeted siRNA for 24 hours. The cells were collected by trypsinization and lysed as described by us previously.<sup>22</sup> Lysate proteins were resolved by sodium dodecyl sulfate-polyacrylamide gel electrophoresis and transferred onto polyvinylidene fluoride membrane. After blocking with a solution consisting of tris-buffered saline supplemented with 0.05% Tween 20% and 5% (w/v) nonfat dry milk, the membrane was exposed to the desired primary antibody overnight at 4°C. Following treatment with an appropriate secondary antibody, immunoreactive bands were visualized using the chemiluminescence method. The blots were stripped and re-probed with anti- $\beta$ -Actin or anti-GAPDH antibody to correct for differences in protein loading. Change in protein level was determined by densitometric scanning of the immunoreactive band using an UN-SCAN-IT gel analysis and graph digitizing software (Version 7.1; Silk Scientific Corporation, Orem, UT) and corrected for  $\beta$ -Actin or GAPDH loading control.

## 2.7 | Determination of cell viability

Cells ( $5 \times 10^4$  cells for PC-3 and LNCaP and  $1.5 \times 10^5$  cells for 22Rv1) were plated in a 12-well plate in triplicate and then treated with DMSO (control) or tested agents with indicated doses for 24 hours. Harvested cells were mixed with trypan blue solution, and then viable cells only were counted on a hemocytometer as described previously.<sup>23</sup>

## 2.8 | Determination of apoptosis

Apoptosis induction was assessed by flow cytometry using Annexin V/propidium iodide (PI) Apoptosis Detection kit or immunoblotting analysis using cleaved PARP and cleaved caspase-3 antibodies. For quantitation of apoptosis by flow cytometry using Annexin V/PI kit, cells were treated with DMSO (control) or tested agents with indicated doses for 24 hours. Cells were harvested and washed with PBS. Cells were suspended in binding buffer and stained with Annexin V and PI solution for 15 minutes at room temperature in the dark. Samples were then diluted with binding buffer. Stained cells were analyzed using the Accuri C6 flow cytometer.

## 2.9 | RNA interference of GABARAPL1

Cells were seeded in six-well plates and transfected at 50% confluency with a control (nonspecific) siRNA or GABARAPL1 siRNA. Twenty-four hours after transfection, the cells were treated with DMSO (control) or 2  $\mu$ M of WA for 24 hours. Cells were then collected and processed for immunoblotting.

## 2.10 | Analysis of The Cancer Genome Atlas data

The University of California Santa Cruz Xena Browser (<http://xena.ucsc.edu/public-hubs/>) was used to analyze changes in gene expression between normal prostate tissues and prostate adenocarcinoma in prostate cancer The Cancer Genome Atlas (TCGA) RNA-seq data set.

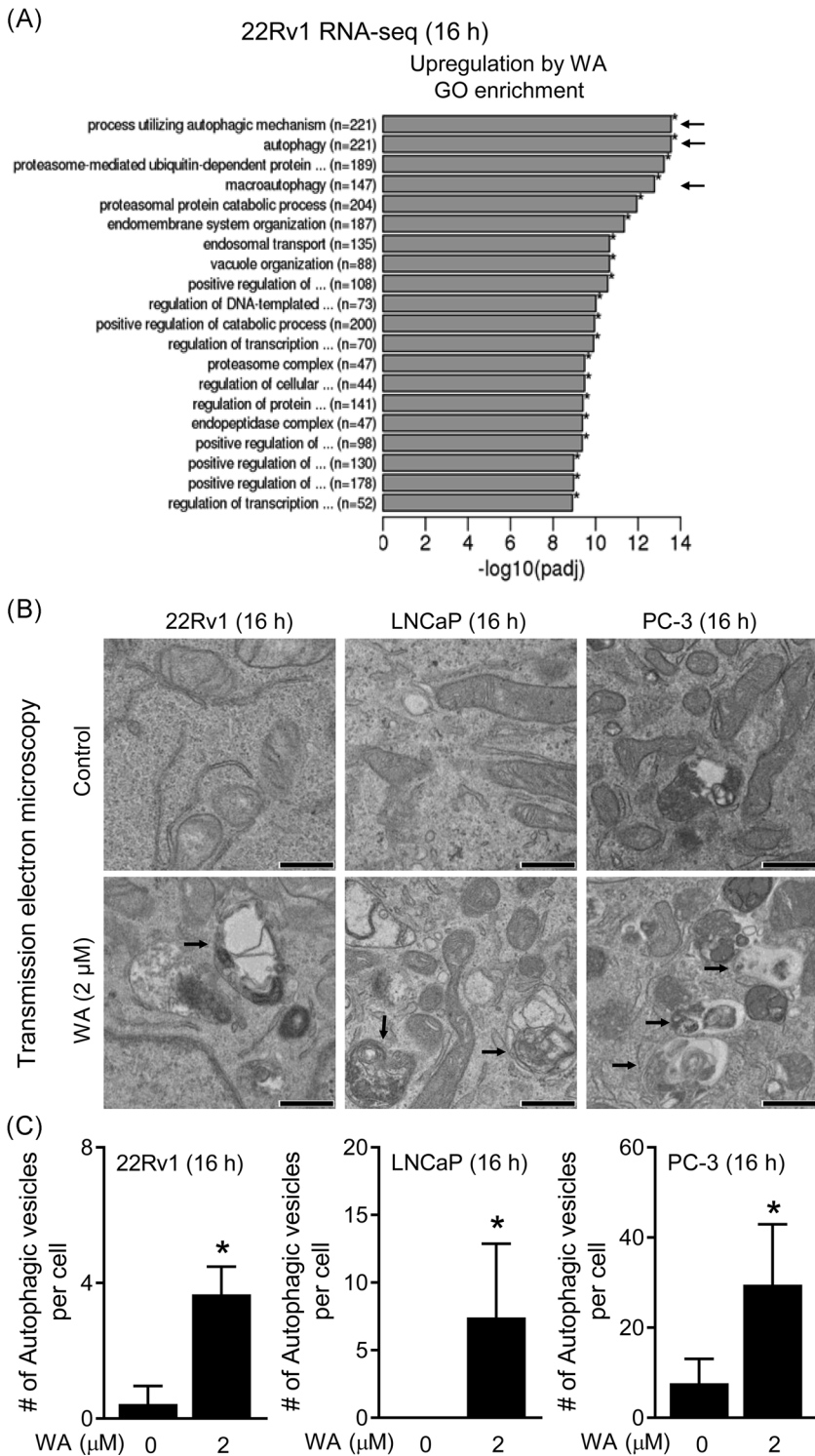
## 2.11 | Statistical analysis

All data were analyzed using the Prism 8 (version 8.0.0.224) of the GraphPad Software (San Diego, CA). Statistical methods used in this study were analysis of variance (ANOVA) followed by Bonferroni's multiple comparison test or unpaired *t* test.  $P < .05$  was considered statistically significant. For gene correlation evaluation, Pearson correlation analysis was used.

# 3 | RESULTS

## 3.1 | WA treatment induced autophagy in human prostate cancer cells

Figure 1A summarizes the GO pathway analysis for upregulated gene sets in a castration-resistant human prostate cancer cell line (22Rv1) upon 16-hour exposure to WA. Most enriched gene sets included process utilizing autophagic mechanism ( $n = 221$ ), autophagy ( $n = 221$ ), and macroautophagy ( $n = 147$ ) (Figure 1A). Among these genes, 95 were selected by fold change with a cut-off of greater than 2 (Table S1). Initially, we performed transmission electron microscopy using 22Rv1,



LNCaP, and PC-3 cells after 16-hour treatment with DMSO (control) or 2  $\mu$ M WA. As indicated by arrows in Figure 1B, autophagic bodies were prominent in WA-treated 22Rv1, LNCaP, and PC-3 cells when compared to vehicle-treated control cells. The numbers of the autophagic bodies were significantly higher in all cell lines following exposure to WA (Figure 1C). Collectively, these results indicated autophagy induction by WA treatment in human prostate cancer cells irrespective of AR status or androgen sensitivity.

**FIGURE 1** WA treatment induces autophagy in human prostate cancer cells. A, GO enrichment analysis showing upregulation of genes following 16-hour treatment of 22Rv1 cells with 2  $\mu$ M WA in comparison with solvent control identified from RNA-seq experiment. The vertical axis shows the description of each term.  $P_{adj}$  defines the adjusted  $P$  value. Arrows indicate autophagy-associated genes. B, Representative transmission electron micrographs (magnification,  $\times 25\,000$ ; scale bar = 600 nm) of 22Rv1, LNCaP, and PC-3 cells after 16-hour treatment with DMSO (control) or 2  $\mu$ M WA. Some autophagic vesicles are indicated by arrows. C, Quantification of the number of autophagic vesicles shown in panel B. Results are shown as mean  $\pm$  SD ( $n = 6-7$ ). \*Significantly different ( $P < .05$ ) compared with DMSO-treated control by unpaired  $t$  test. DMSO, dimethyl sulfoxide; GO, Gene Ontology; WA, withaferin A

### 3.2 | WA treatment modulated expression of autophagy-related genes in 22Rv1 cells

We next performed a targeted array in control and WA-treated 22Rv1 cells (8- or 16-hour exposure) using RT<sup>2</sup> Profiler PCR Array containing 84 human autophagy-related genes. Figure 2A displays Venn diagram showing common and unique genes in 22Rv1 cells following 8- or 16-hour exposure to WA compared with corresponding DMSO-treated

control (threshold cut-off  $-1.5$ -fold and  $P < .05$ ). Upregulated and downregulated genes by WA treatment at each time point can be visualized in the heatmap (Figure 2B). In Figure 2C,D, relative gene expression in response to WA for 8 or 16 hours compared with corresponding DMSO-treated control are plotted. Fourteen genes in

bold were commonly altered by WA exposure at both time points. Among the 14 genes, 3 genes including *BAD*, *DRAM1*, and *ATG16L2* were downregulated and the remaining 11 common genes (*ATG4A*, *WIP1*, *HSP90AA1*, *EIF2AK3*, *HSPA8*, *ATG9B*, *FAS*, *SQSTM1*, *NPC1*, *MAP1LC3B*, and *GABARAPL1*) were upregulated by WA treatment (Table S2).

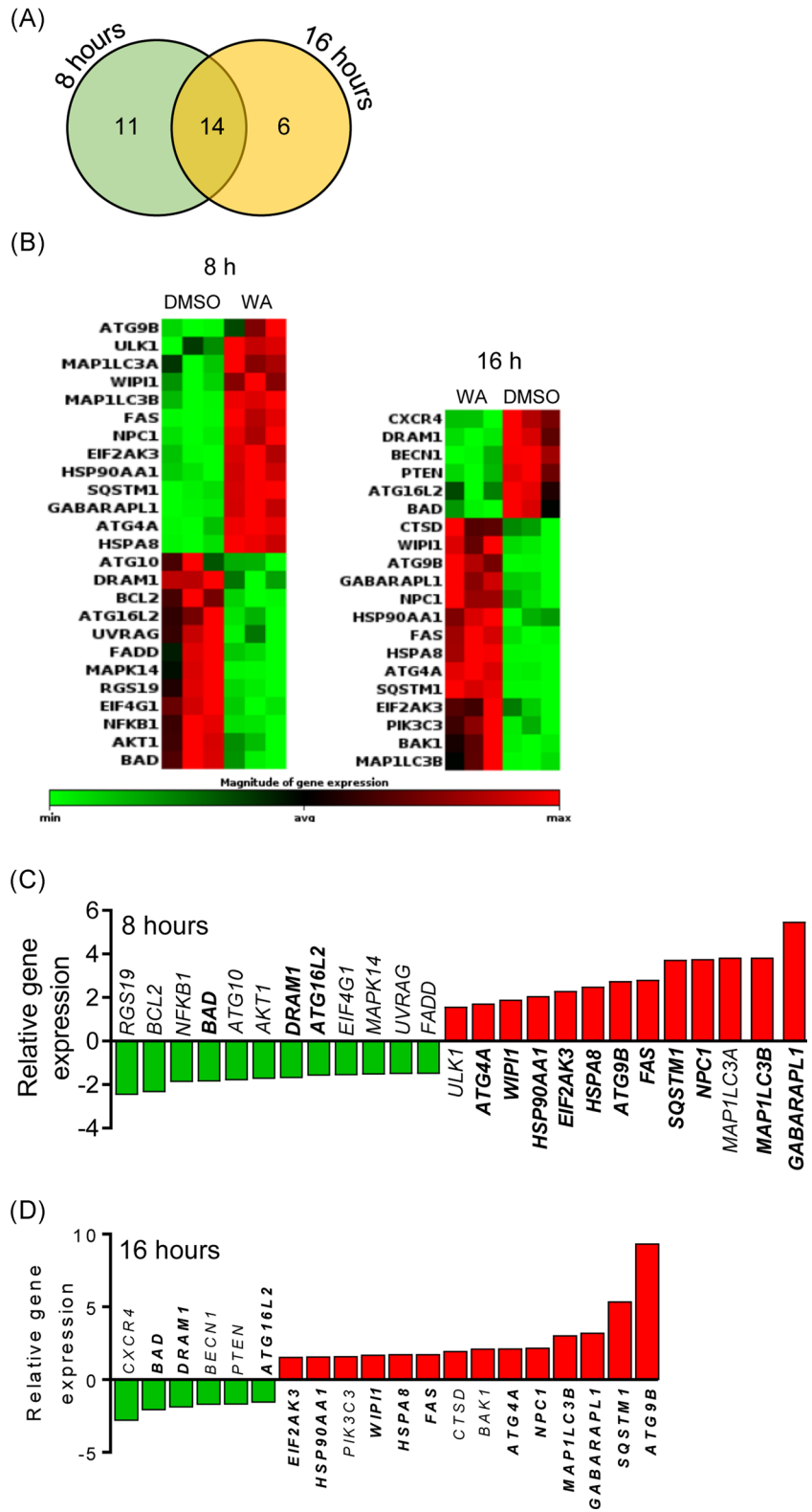


**FIGURE 2** WA alters the expression of genes associated with autophagy in 22Rv1 human prostate cancer cells. A, Venn diagram showing unique and overlapping genes between 8- and 16-hour WA-treated 22Rv1 cells identified from RT<sup>2</sup> Profiler PCR Array (Human Autophagy) experiment. B, Heat maps of the differentially expressed genes in control and WA-treated 22Rv1 cells (n = 3) for 8 or 16 hours. C and D, Relative gene expression in response to WA treatment for (C) 8 hours and (D) 16 hours in 22Rv1 cells. The cut-off value was set to  $\pm 1.5$ -fold change in expression by WA treatment at  $P < .05$ . DMSO, dimethyl sulfoxide; WA, withaferin A [Color figure can be viewed at [wileyonlinelibrary.com](http://wileyonlinelibrary.com)]

### 3.3 | Comparison of RNA-seq data and RT<sup>2</sup> Profiler PCR array results

We compared the expression pattern of 14 common genes identified from the human autophagy PCR array with those in 22Rv1 RNA-seq results (Table S3). The RNA-seq data and PCR array results were consistent for all genes except *DRAM1* (Figure 3A,B). Because LC3BII is a key autophagy marker, we next examined whether WA upregulates LC3BII protein in human prostate cancer cell lines with different genetic backgrounds. As seen in Figure 3C, 2 μM WA treatment robustly induced LC3BII protein expression in 22Rv1, LNCaP, and PC-3 cells. For autophagy flux evaluation, prostate cancer cells were treated with DMSO (control) or 2 μM WA for 24 hours in the absence

or presence of autophagy inhibitor BafA1 which interferes with the fusion of autophagosomes with lysosome. Interestingly, WA treatment induced both SQSTM1 and LC3BII expression in all three cell lines, and the addition of BafA1 led to augmentation of their accumulation by blocking lysosomal degradation of both SQSTM1 and LC3BII proteins (Figure 3C,D). Because SQSTM1 is degraded when autophagy is induced, the SQSTM1 increase in response to WA was not expected but explainable. SQSTM1 is not only a well-known autophagic adaptor protein but also a multifunctional protein participating in protein aggregation and degradation and regulating cellular signaling.<sup>24</sup> The expression of SQSTM1 is also transcriptionally regulated by NF-E2-related factor 2 (NRF2) by binding to the antioxidant responsive element (ARE) motif found in the promoter of

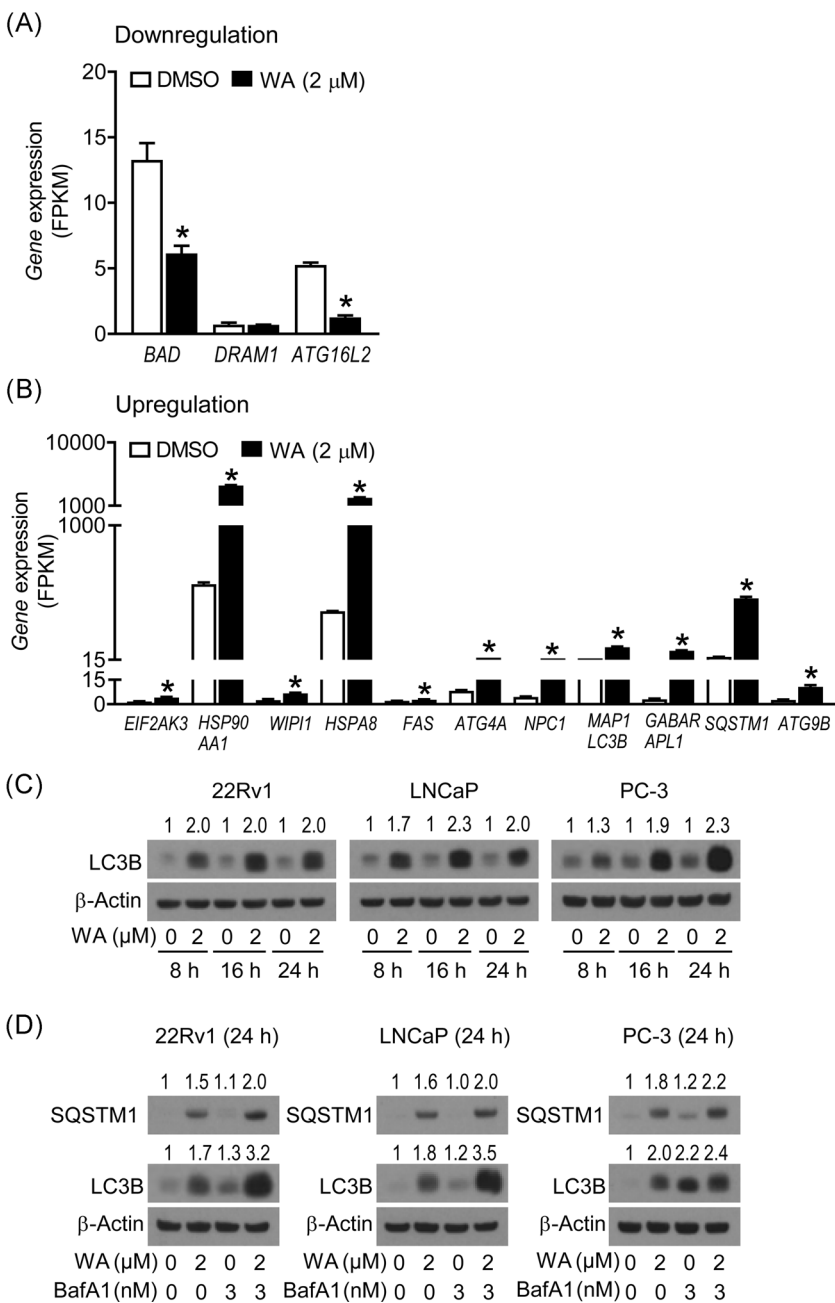


**FIGURE 3** RNA-seq data confirm(s) the common autophagy genes modulated by WA treatment from RT<sup>2</sup> Profiler PCR Array results. A and B, Gene expression (FPKM) from RNA-seq for (A) downregulation and (B) upregulation of common autophagy genes in response to WA treatment from RT<sup>2</sup> Profiler PCR Array results. Results are shown as mean ± SD (n = 3). \*Significantly different (P < .05) compared with DMSO-treated control by unpaired t test. C, Immunoblotting for LC3B and β-Actin in lysates from 22Rv1, LNCaP, and PC-3 cells after treatment with DMSO (control) or 2 μM WA for indicated time periods. Number above bands indicates relative protein expression compared with corresponding DMSO-treated control. Experiments were repeated at least twice with comparable results. D, Immunoblotting for SQSTM1, LC3B, and β-Actin in lysates from 22Rv1, LNCaP, and PC-3 cells after 24-hour treatment with DMSO (control) or 2 μM WA in the absence or presence of 3 nM BafA1. Number above bands indicates relative protein expression compared with corresponding DMSO-treated control. Experiments were repeated at least twice with comparable results. DMSO, dimethyl sulfoxide; WA, withaferin A

SQSTM1.<sup>24</sup> As WA functions as an inducer of NRF2,<sup>25</sup> induction of SQSTM1 expression in WA-treated cells is complex.

### 3.4 | WA-induced autophagy was cytoprotective

To determine the functional significance of autophagy, we performed cell viability assays using 22Rv1, LNCaP, and PC-3 cells (Figure 4). The cells were treated for 24 hours with DMSO (control) or 2  $\mu$ M WA in the presence or absence of autophagy inhibitors including 3-MA and BafA1. As can be seen in Figure 4, 2  $\mu$ M WA reduced the viability of all three prostate cancer cells. The WA-mediated cell viability suppression in 22Rv1 and LNCaP cells was relatively more pronounced than in the PC-3 cells. 3-MA did not show any effect on WA-mediated decrease in viability of any cell line. However, BafA1 itself decreased the cell viability and augmented WA's cytotoxicity in all cell lines. Both 3-MA and BafA1 are autophagy inhibitors but affect different phases of autophagy. The 3-MA prevents the formation of autophagosome, early autophagy phase, by inhibiting class III phosphatidylinositol 3-kinase activity, while BafA1 blocks fusion of autophagosomes with lysosomes by inhibiting vacuolar H<sup>+</sup>-ATPase.

### 3.5 | Autophagy inhibition augmented WA-induced apoptosis in prostate cancer cells

Because cell viability inhibition by WA was increased in the presence of BafA1, we examined the effect of combined treatment with WA and BafA1 on apoptosis induction. Figure 5A shows histograms of Annexin V and PI staining for live cells (Annexin V<sup>-</sup> and PI<sup>-</sup>), early apoptotic population (Annexin V<sup>+</sup> and PI<sup>-</sup>), late apoptotic fraction (Annexin V<sup>+</sup> and PI<sup>+</sup>), or necrotic (Annexin V<sup>-</sup> and PI<sup>+</sup>) cells after 24-hour treatment with DMSO (control) or 2  $\mu$ M WA in the presence or absence of 3 nM BafA1. As expected, WA treatment increased total (early + late) apoptotic fraction in 22Rv1 (Figure 5B) and LNCaP (Figure 5C) cells. Co-treatment with BafA1 significantly elevated WA-induced total apoptosis in 22Rv1 and LNCaP cells (Figure 5B,C). In PC-3 cells, 2  $\mu$ M WA alone did not induce apoptosis. However, combined treatment with WA and BafA1 induced total apoptosis in PC-3 cells (Figure 5D). Taken together, these results indicated that WA-mediated autophagy was cytoprotective in human prostate cancer cells.

### 3.6 | Analysis of TCGA data set for expression of autophagy-related genes altered by WA treatment

We examined the prostate cancer TCGA RNA-seq data for expression of genes modulated by WA treatment. The expression of both *BAD* and *ATG16L2*, which were downregulated by WA, were higher in prostate tumors compared with normal prostate tissues (Figure S1A). The expression of *DRAM1* was lower in prostate tumors compared with normal prostate. Four out of the 11 genes that were upregulated by WA treatment were significantly overexpressed in prostate

tumors when compared with normal prostate tissues (Figure S1B). *WIPI1* expression was not different between normal prostate tissues and prostate tumors (Figure S1B). On the other hand, the expression of six genes upregulated by WA treatment were significantly lower in

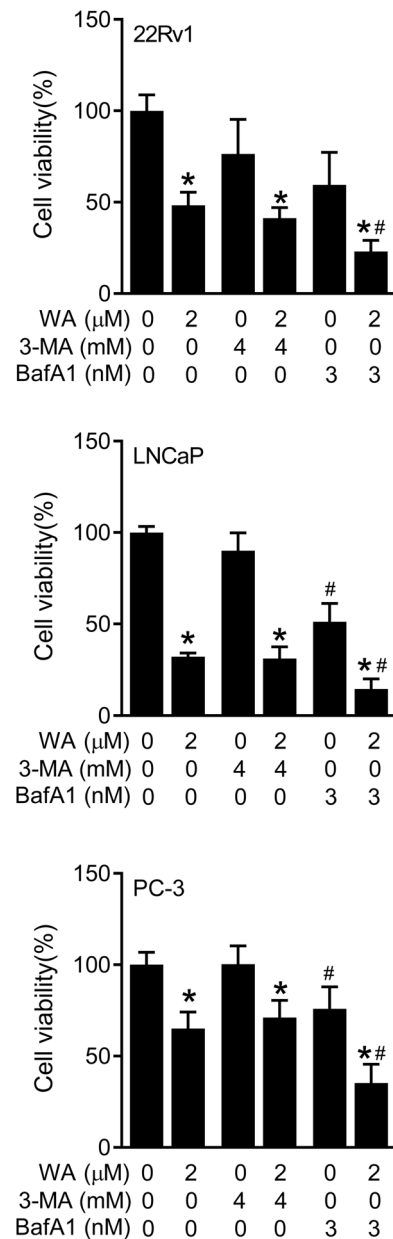


**FIGURE 4** Inhibition of autophagy by BafA1 increases the cytotoxic effect of WA in human prostate cancer cells. Viability of 22Rv1, LNCaP, and PC-3 cells after 24-hour treatment with DMSO (control) or 2  $\mu$ M WA in the absence or presence of 4 mM 3-MA or 3 nM BafA1. Results are shown as mean  $\pm$  SD (n = 3). Significantly different ( $P < .05$ ) compared with \*corresponding DMSO-treated control or #between WA alone and WA + 3-MA or WA alone and WA + BafA1 by one-way ANOVA with Bonferroni's multiple comparison test. Experiments were repeated twice with comparable results. 3-MA, 3-methyl adenine; ANOVA, analysis of variance; DMSO, dimethyl sulfoxide; WA, withaferin A

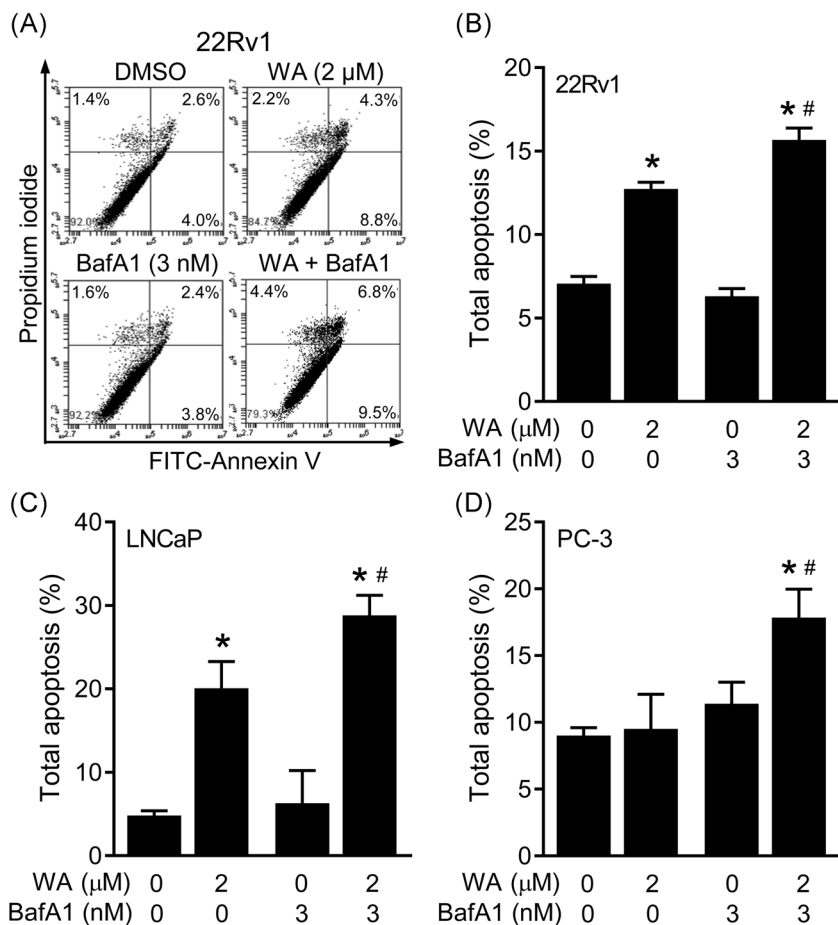


**FIGURE 5** BafA1 augments WA-induced apoptosis in prostate cancer cells. A, Representative histogram of Annexin V and PI staining indicating percentage of live, apoptotic, or necrotic cells in 22Rv1 cells after 24-hour treatment with DMSO (control) or 2 μM WA in the absence or presence of 3 nM BafA1. Quantification of apoptosis in (B) 22Rv1, (C) LNCaP, and (D) PC-3 cells after 24-hour treatment with DMSO (control) or 2 μM WA in the absence or presence of 3 nM BafA1. Results are shown as mean ± SD (n = 3). Significantly different ( $P < .05$ ) compared with \*corresponding DMSO-treated control or #between WA alone and WA + BafA1 by one-way ANOVA with Bonferroni's multiple comparison test. Experiments were repeated twice with comparable results. ANOVA, analysis of variance; DMSO, dimethyl sulfoxide; PI, propidium iodide; WA, withaferin A

prostate tumors, which included *HSP90AA1*, *FAS*, *NPC1*, *MAP1LC3B*, *GABARAPL1*, and *SQSTM1* (Figure S1B).

### 3.7 | Knockdown of GABARAPL1 attenuated proapoptotic potential of WA in human prostate cancer cells

Consistent with RNA-seq results in WA-treated 22Rv1 cells, immunoblotting revealed induction of GABARAPL1 protein upon WA treatment in 22Rv1, LNCaP, and PC-3 cells (Figure 6A). As shown in Figure 6B, WA treatment increased both SQSTM1 and LC3BII expression level in control siRNA-transfected cells. This effect was augmented in GABARAPL1 siRNA-transfected cells suggesting GABARAPL1 as a regulator of WA-induced autophagy flux at least in 22Rv1 prostate cancer cells (Figure 6B). We further examined the effect of GABARAPL1 on WA-induced apoptosis in prostate cancer cells. As expected, WA alone induced apoptosis indicated by an increase in PARP cleavage and cleaved caspase-3 level in control siRNA-transfected cells (Figure 6C). However, this effect was diminished in GABARAPL1 siRNA-transfected 22Rv1 cells indicating the proapoptotic role of GABARAPL1 in WA-induced apoptosis at least in 22Rv1 cells. Because WA is known to produce reactive oxygen species (ROS) in prostate cancer cells and ROS is involved in

autophagy regulation,<sup>18,26</sup> we checked the effect of an antioxidant on WA-mediated autophagy. A synthetic superoxide dismutase and catalase mimetic EUK134 was used for these experiments. 22Rv1 cells were treated with DMSO (control) or 2 μM WA in the absence or presence of 30 μM EUK134 for 8, 16, or 24 hours. As shown in Figure 6D, the WA-mediated increase in SQSTM1 or LC3BII was not affected by EUK134. These results indicated that WA-induced autophagy was not triggered by ROS production.

## 4 | DISCUSSION

In the present study, we show that WA induces autophagy in human prostate cancer cells and the net outcome of this effect is cytoprotective. We also show that WA-induced autophagy is not a cell line-specific response but instead a consistent pharmacological effect in prostate cancer cells with distinct genetic backgrounds. We also observed induction of *HSPA8* and *HSP90AA1* expression by WA treatment in 22Rv1 cells. These proteins are known to regulate chaperone-mediated autophagy in cooperation with LAMP2A.<sup>27</sup> Therefore, chaperone-mediated autophagy could be responsible for WA-mediated cytoprotective response in prostate cancer cells.

ROS production has diverse effects in the context of cancer including DNA damage and effect on activities of oncogenes and

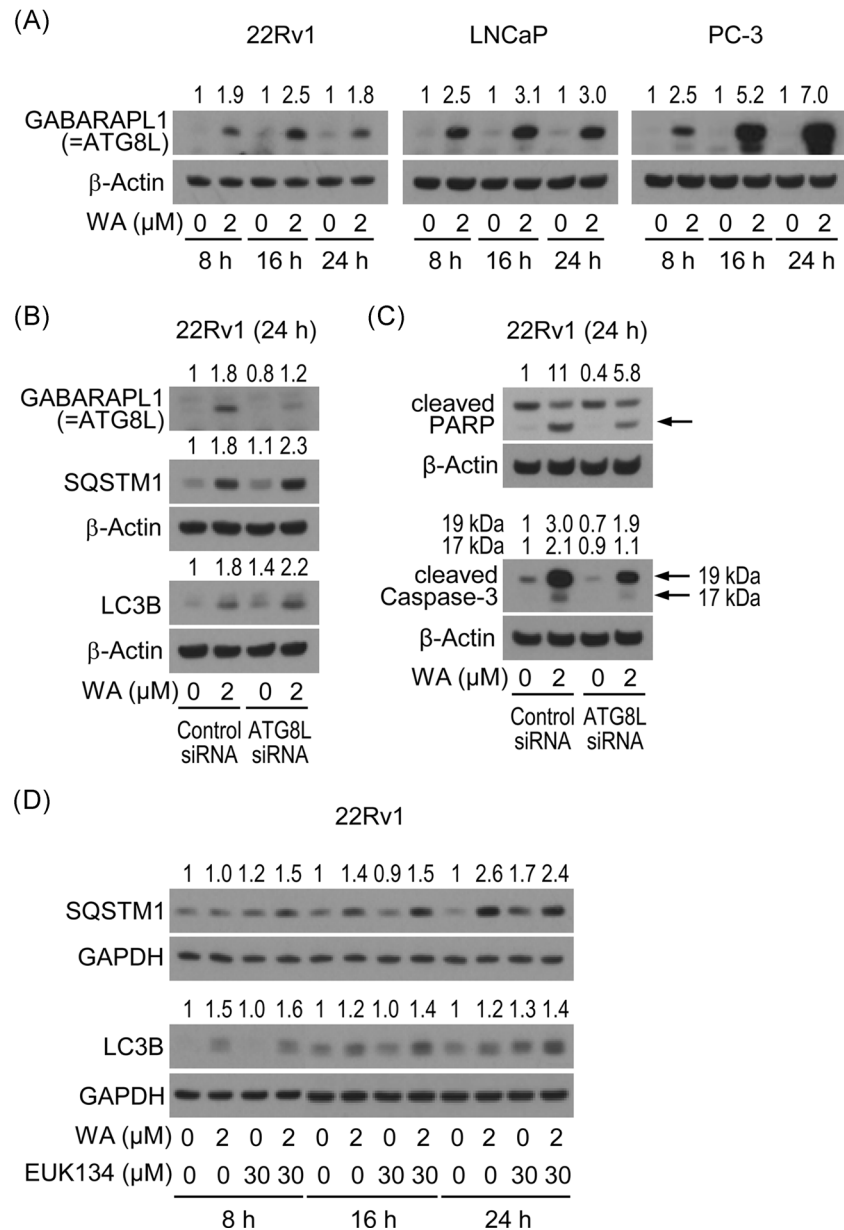


**FIGURE 6** WA treatment elevates GABARAPL1/ATG8L expression in human prostate cancer cells. A, Immunoblotting for GABARAPL1/ATG8L and  $\beta$ -Actin proteins in 22Rv1, LNCaP, and PC-3 cells treated with DMSO (control) or 2  $\mu$ M WA for indicated time periods. Numbers on top of bands are fold change in protein level relative to corresponding DMSO-treated control. Experiments were repeated twice with comparable results. Immunoblotting for (B) GABARAPL1/ATG8L, SQSTM1, LC3B, and  $\beta$ -Actin proteins or (C) cleaved PARP, cleaved caspase-3, and  $\beta$ -Actin proteins in 22Rv1 cells transiently transfected with control siRNA or GABARAPL1/ATG8L-targeted siRNA for 24 hours and then treated with DMSO (control) or 2  $\mu$ M WA for 24 hours. Numbers on top of bands are fold change in protein level relative to DMSO-treated control siRNA-transfected 22Rv1 cells. The experiment was repeated at least twice with consistent results. Arrows indicated right band for cleaved PARP or cleaved caspase-3. D, Immunoblotting for SQSTM1, LC3B, and GAPDH in 22Rv1 cells treated with DMSO (control) or 2  $\mu$ M WA in the absence or presence of 30  $\mu$ M EUK134 for indicated time periods. Numbers on top of bands are fold change in protein level relative to corresponding DMSO-treated 22Rv1 cells in the absence of EUK134. The experiment was repeated twice with consistent results. DMSO, dimethyl sulfoxide; GAPDH, glyceraldehyde 3-phosphate dehydrogenase; PARP, poly(ADP-ribose) polymerase; siRNA, small interfering RNA; WA, withaferin A

tumor suppressors. ROS and oxidative stress levels can vary according to the cancer grade and could lead to a differential response.<sup>28</sup> Studies have indicated that oxidative stress can cause an activating mutation of Ras proto-oncogene but inhibit p53 tumor suppressor.<sup>28</sup> ROS production is suggested to promote

carcinogenesis via epigenetic alterations in tumor-suppressor genes like retinoblastoma and Von Hippel-Lindau, and by modulating activities of diverse signaling proteins including mitogen-activated protein kinase, extracellular regulated kinase, nuclear factor- $\kappa$ B, and so forth.<sup>28</sup> Thus, ROS can regulate the activities of

cancer-related pathways, via direct and indirect mechanisms. WA-induced apoptosis in prostate cancer cells is dependent on ROS production.<sup>18</sup> A role for ROS in induction of autophagy has also been shown.<sup>26</sup> It is interesting to note that WA-induced autophagy in prostate cancer cells is not altered in the presence of an antioxidant. Instead, we found a critical role for GABARAPL1 in regulation of WA-induced apoptosis. Cleavage of both PARP and caspase-3 resulting from WA exposure is attenuated by RNA interference of GABARAPL1. It is important to point out that WA treatment caused maximum induction of GABARAPL1 gene at the 8-hour time point. Literature data is mixed with regard to precise role of GABARAPL1 in prostate cancer. One study showed that growth of AR-positive (LNCaP) as well as CRPC (22Rv1) cells were inhibited by GABARAPL1 knockdown that was associated with a decrease in AR/AR-V transcription and nuclear translocation of AR.<sup>29</sup> Pulldown assay showed direct interaction between AR/AR-V and GABARAPL1.<sup>29</sup> Moreover, GABARAPL1 expression was negatively associated with 5 years survival in the Oncomine data set for prostate cancer.<sup>29</sup> On the other hand, this protein was shown to counteract PI3K/Akt pathway leading to suppression of metastasis.<sup>30</sup> Moreover, GABARAPL1 downregulation in prostate cancer tissues was associated with decreased disease-free survival in prostate cancer patients.<sup>30</sup> The present study reveals that WA causes induction of GABARAPL1 and its knockdown inhibits WA-mediated apoptosis.

The LNCaP cell line, which is androgen-responsive, was relatively more sensitive to apoptosis induction by WA when compared to castration-resistant 22Rv1 cells (Figure 5B-C). At the same time, the extent of autophagy induction was comparable in LNCaP and 22Rv1 cells (Figure 1C). The mechanism for differential sensitivity of the prostate cancer cells to WA-mediated apoptosis is not yet clear. Apoptosis induction by other natural products is associated with the downregulation of AR expression.<sup>31</sup> WA treatment also downregulates AR expression.<sup>14</sup> Therefore, it is possible that AR expression may affect apoptosis induction by WA in prostate cancer cells, but further work is needed to test this hypothesis.

In summary, the present study reveals that WA treatment induces cytoprotective autophagy in prostate cancer cells. WA treatment also affected the expression of many other autophagy-related genes. Some of them are associated with the canonical autophagy pathway, including ATG16L2, WIPI1, ATG4A, and ATG9B. Further work is necessary to determine if WA-induced apoptosis is also increased by knockdown of these proteins.

## ACKNOWLEDGMENTS

This study was supported by Grants RO1 CA142604-10 and RO1 CA225716-1A1 awarded by the National Cancer Institute (S. V. Singh). This study used the Flow Cytometry Facility and Cell and Tissue Imaging Facility supported in part by the UPMC Hillman Cancer Center Support Grant from the National Cancer Institute (P30 CA047904).

## CONFLICT OF INTERESTS

The authors declare that there are no conflict of interests.

## DATA AVAILABILITY STATEMENT

All data will be shared upon request.

## ORCID

Shivendra V. Singh  <http://orcid.org/0000-0002-3733-144X>

## REFERENCES

- Siegel RL, Miller KD, Jemal A. Cancer statistics, 2020. *CA Cancer J Clin*. 2020;70:7-30.
- Mansinho A, Macedo D, Fernandes I, Costa L. Castration-resistant prostate cancer: mechanisms, targets and treatment. *Adv Exp Med Biol*. 2018;1096:117-133.
- Nguyen HG, Yang JC, Kung HJ, et al. Targeting autophagy overcomes Enzalutamide resistance in castration-resistant prostate cancer cells and improves therapeutic response in a xenograft model. *Oncogene*. 2014;33:4521-4530.
- Liu Y, Zuckier LS, Ghesani NV. Dominant uptake of fatty acid over glucose by prostate cells: a potential new diagnostic and therapeutic approach. *Anticancer Res*. 2010;30:369-374.
- Ziparo E, Petrungraro S, Marini ES, et al. Autophagy in prostate cancer and androgen suppression therapy. *Int J Mol Sci*. 2013;14:12090-12106.
- Itkonen HM, Brown M, Urbanucci A, et al. Lipid degradation promotes prostate cancer cell survival. *Oncotarget*. 2017;8:38264-38275.
- Barakat DJ, Friedman AD. Autophagy is required for PTEN-loss driven prostate cancer. *Transl Cancer Res*. 2016;5(suppl 4):725-729.
- Farrow JM, Yang JC, Evans CP. Autophagy as a modulator and target in prostate cancer. *Nat Rev Urol*. 2014;11:508-516.
- Thompson IM Jr, Goodman PJ, Tangen CM, et al. Long-term survival of participants in the prostate cancer prevention trial. *N Engl J Med*. 2013;369:603-610.
- Andriole GL, Bostwick DG, Brawley OW, et al. Effect of dutasteride on the risk of prostate cancer. *N Engl J Med*. 2010;362:1192-1202.
- Klein EA, Thompson IM Jr, Tangen CM, et al. Vitamin E and the risk of prostate cancer: the Selenium and Vitamin E Cancer Prevention Trial (SELECT). *JAMA*. 2011;306:1549-1556.
- Dutta R, Khalil R, Green R, Mohapatra SS, Mohapatra S. *Withania somnifera* (Ashwagandha) and withaferin A: potential in integrative oncology. *Int J Mol Sci*. 2019;20:5310.
- Yang H, Shi G, Dou QP. The tumor proteasome is a primary target for the natural anticancer compound withaferin A isolated from "Indian winter cherry". *Mol Pharmacol*. 2007;71:426-437.
- Srinivasan S, Ranga RS, Burikhanov R, Han SS, Chendil D. Par-4-dependent apoptosis by the dietary compound withaferin A in prostate cancer cells. *Cancer Res*. 2007;67:246-253.
- Roy RV, Suman S, Das TP, Luevano JE, Damodaran C. Withaferin A, a steroidal lactone from *Withania somnifera*, induces mitotic catastrophe and growth arrest in prostate cancer cells. *J Nat Prod*. 2013;76:1909-1915.
- Suman S, Das TP, Moselhy J, et al. Oral administration of withaferin A inhibits carcinogenesis of prostate in TRAMP model. *Oncotarget*. 2016;7:53751-53761.
- Moselhy J, Suman S, Alghamdi M, et al. Withaferin A inhibits prostate carcinogenesis in a PTEN-deficient mouse model of prostate cancer. *Neoplasia*. 2017;19:451-459.
- Nishikawa Y, Okuzaki D, Fukushima K, et al. Withaferin A induces cell death selectively in androgen-independent prostate cancer cells but not in normal fibroblast cells. *PLOS One*. 2015;10:e0134137.

19. Rah B, ur Rasool R, Nayak D, et al. PAWR-mediated suppression of BCL2 promotes switching of 3-azido withaferin A (3-AWA)-induced autophagy to apoptosis in prostate cancer cells. *Autophagy*. 2015;11:314-331.
20. Kim SH, Hahm ER, Singh KB, Shiva S, Stewart-Ornstein J, Singh SV. RNA-seq reveals novel mechanistic targets of withaferin A in prostate cancer cells. *Carcinogenesis*. 2020;41:778-789.
21. Singh SV, Srivastava SK, Choi S, et al. Sulforaphane-induced cell death in human prostate cancer cells is initiated by reactive oxygen species. *J Biol Chem*. 2005;280:19911-19924.
22. Xiao D, Srivastava SK, Lew KL, et al. Allyl isothiocyanate, a constituent of cruciferous vegetables, inhibits proliferation of human prostate cancer cells by causing G<sub>2</sub>/M arrest and inducing apoptosis. *Carcinogenesis*. 2003;24:891-897.
23. Xiao D, Choi S, Johnson DE, et al. Diallyl trisulfide-induced apoptosis in human prostate cancer cells involves c-Jun N-terminal kinase and extracellular-signal regulated kinase-mediated phosphorylation of Bcl-2. *Oncogene*. 2004;23:5594-5606.
24. Su H, Wang X. p62 Stages an interplay between the ubiquitin-proteasome system and autophagy in the heart of defense against proteotoxic stress. *Trends Cardiovasc Med*. 2011;21:224-228.
25. Palliyaguru DL, Chartoumpakis DV, Wakabayashi N, et al. Withaferin A induces Nrf2-dependent protection against liver injury: role of Keap1-independent mechanisms. *Free Radic Biol Med*. 2016;101:116-128.
26. Gibson SB. Investigating the role of reactive oxygen species in regulating autophagy. *Methods Enzymol*. 2013;528:217-235.
27. Pajares M, Rojo AI, Arias E, Díaz-Carretero A, Cuervo AM, Cuadrado A. Transcription factor NFE2L2/NRF2 modulates chaperone-mediated autophagy through the regulation of LAMP2A. *Autophagy*. 2018;14:1310-1322.
28. Miyata Y, Matsuo T, Sagara Y, Ohba K, Ohyama K, Sakai H. A mini-review of reactive oxygen species in urological cancer: correlation with NADPH oxidases, angiogenesis, and apoptosis. *Int J Mol Sci*. 2017;18:2214.
29. Su B, Zhang L, Liu S, Chen X, Zhang W. GABARAPL1 promotes AR+ prostate cancer growth by increasing FL-AR/AR-V transcription activity and nuclear translocation. *Front Oncol*. 2019;9:1254.
30. Su W, Li S, Chen X, et al. GABARAPL1 suppresses metastasis by counteracting PI3K/Akt pathway in prostate cancer. *Oncotarget*. 2017;8:4449-4459.
31. Culig Z, Santer FR. Androgen receptor signaling in prostate cancer. *Cancer Metastasis Rev*. 2014;33:413-427.

#### SUPPORTING INFORMATION

Additional supporting information may be found online in the Supporting Information section.

**How to cite this article:** Hahm E-R, Singh SV. Cytoprotective autophagy induction by withaferin A in prostate cancer cells involves GABARAPL1. *Molecular Carcinogenesis*. 2020;1–11. <https://doi.org/10.1002/mc.23240>